

Atom Interferometers with Scalable Enclosed Area

Holger Müller,^{1,2,*} Sheng-wei Chiow,³ Sven Herrmann,³ and Steven Chu^{1,2}

¹*Department of Physics, 366 Le Conte Hall, University of California, Berkeley, California 94720-7300, USA*

²*Lawrence Berkeley National Laboratory, One Cyclotron Road, Berkeley, California 94720, USA*

³*Physics Department, Stanford University, 382 Via Pueblo Mall, Stanford, California 94305, USA*

(Received 24 March 2009; published 18 June 2009)

Bloch oscillations (i.e., coherent acceleration of matter waves by an optical lattice) and Bragg diffraction are integrated into light-pulse atom interferometers with large momentum splitting between the interferometer arms, and hence enhanced sensitivity. Simultaneous acceleration of both arms in the same internal states suppresses systematic effects, and simultaneously running a pair of interferometers suppresses the effect of vibrations. Ramsey-Bordé interferometers using four such Bloch-Bragg-Bloch beam splitters exhibit 15% contrast at $24\hbar k$ splitting, the largest so far ($\hbar k$ is the photon momentum); single beam splitters achieve $88\hbar k$. The prospects for reaching 100 s of $\hbar k$ and applications such as gravitational wave sensors are discussed.

DOI: 10.1103/PhysRevLett.102.240403

PACS numbers: 03.75.Dg, 37.25.+k, 67.85.-d

Light-pulse atom interferometers use the momentum transfer in light-atom interactions to split and reflect matter waves, thus forming the interferometer arms [1]. They have been used for accurate and high precision measurements of gravity [2], the fine-structure constant [3–5], gravity gradients [6], Newton’s gravitational constant [7,8], and one of the few terrestrial tests of general relativity that is competitive with astrophysics [9]. In these examples, the atom-light interactions are Raman transitions which transfer the momentum $\Delta p = 2\hbar k$ of two photons. This limits the space-time area enclosed between the interferometer arms, and hence the sensitivity. Bragg diffraction of matter waves has been used to increase Δp [10], the current record being $24\hbar k$ [11,12]. Unfortunately, this number represents a technical limit, as the required laser power increases sharply with Δp [13]. Bloch oscillations [5,14,15] or adiabatic transfer [3,4] have been used to transfer thousands of $\hbar k$, but so far only to the common momentum of the interferometer arms, which does not increase the enclosed area. Here, we use them to increase the splitting of the arms and thus increase the enclosed area (Fig. 1). Bragg beam splitters are embedded between Bloch oscillations to achieve a Δp of up to $88\hbar k$. In Ramsey-Bordé interferometers with $\Delta p = 24\hbar k$, we see interferences with $\sim 15\%$ contrast (compared to 4% with Bragg diffraction [11]). The enclosed area is no longer limited by available laser power. This work is thus the first demonstration of an interferometer whose enclosed area can be scaled up to allow for proposed landmark experiments such as detection of low-frequency gravitational waves [16] or the Lense-Thirring effect [17], tests of the equivalence principle at sensitivities of up to $\delta g/g \sim 10^{-17}$ [18], atom neutrality [19], or measurements of fundamental constants with sensitivity to supersymmetry [20].

The two basic ingredients of this work are Bragg diffraction of matter waves at an optical lattice and Bloch

oscillations of matter waves in an accelerated optical lattice. To describe them, we consider an atom of mass M in the electric fields of two counterpropagating laser beams whose frequencies are ω_1 and ω_2 . We denote $k = (\omega_1 + \omega_2)/(2c)$ the average wave number.

For Bragg diffraction [13], ω_1 and ω_2 are constant in the rest frame of the atom. Neglecting spontaneous processes, the atom absorbs n photons at ω_1 from one beam and is stimulated to emit n into the other beam at ω_2 . The atom emerges in its original internal quantum state but moving with a momentum of $2n\hbar k$ and a kinetic energy of $(2n\hbar k)^2/(2M) \equiv 4n^2\hbar\omega_r$, where ω_r is the recoil frequency. This must match the energy $n\hbar(\omega_1 - \omega_2)$ lost by the laser field, which determines the Bragg diffraction order n . To make a beam splitter for matter waves, the pulse duration and intensity are chosen such that the process happens with a probability of 1/2 (a “ $\pi/2$ ”-pulse).

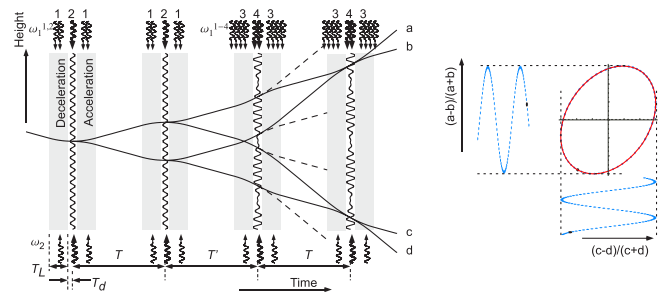


FIG. 1 (color online). Left: space-time diagram of simultaneous conjugate Ramsey-Bordé BBB-interferometers. 1: Dual optical lattice; 2: single Bragg beam splitter; 3: quadruple optical lattice; 4: dual Bragg beam splitter; (a)–(d): outputs. The dashed lines indicate trajectories that do not interfere. Right: plotting the outputs of the interferometers versus one another draws an ellipse.

For Bloch oscillations, suppose the beams initially have zero difference frequency, which is then ramped linearly with time, $\omega_1 - \omega_2 = \dot{\omega}t$. At a certain time, it will thus satisfy the Bragg resonance condition for transitions between momentum states $|p = 0\rangle \rightarrow |p = 2\hbar k\rangle$ and then subsequently $|p = 2\hbar k\rangle \rightarrow |p = 4\hbar k\rangle, \dots$. The atom thus receives $2\hbar k$ of momentum in intervals given by the Bloch period $\tau_B = 8\omega_r/\dot{\omega}$. Theory and experiment show that when $\dot{\omega}$ satisfies an adiabaticity criterion [14] and the difference frequency is held constant after it reaches $\omega_1 - \omega_2 = 8N\omega_r$, where $N = 1, 2, 3, \dots$, the population emerges in an $|p = 2N\hbar k\rangle$ momentum state which is nearly pure [14].

The simplest way to increase the momentum transfer of a beam splitter with Bloch oscillations would be to take one output of a conventional beam splitter and accelerate it with Bloch oscillations [21]; a total momentum splitting of $10\hbar k$ has been achieved [22] with a contrast at the few-percent level. According to simulations, parameters like the lattice depth and acceleration can be chosen such that the other arm can remain unaccelerated if the initial momentum splitting is sufficient [23]. In this configuration, however, the lattice causes an imbalance in the ac Stark effect between arms. This can easily contribute tens of radians to the interferometer phase as a function of the lattice depth. Even if this can be cancelled between subsequent optical lattices [22], fluctuations or drift in the laser power, and hence the lattice depth, may spoil the mrad precision [2] of typical interferometers.

To minimize this systematic effect, it is better to simultaneously accelerate both arms with a pair of lattices. This will balance the ac Stark effect. The balance can be maintained by controlling the intensity balance of the lattice beams, which is technically much easier than accurate control of their absolute intensity. The final version of our beam splitter also has a pair of Bloch oscillations at the input, which decelerate the relative velocity of the arms. This leads to symmetry with respect to interchanging inputs and outputs, facilitating use in atom interferometers.

Figure 2 shows our final configuration, which we may call the Bloch-Bragg-Bloch (BBB) beam splitter. Consider the first and second beam splitter of Fig. 1. Initially, its two atomic inputs have a momentum difference of $(2n + 4N)\hbar k$. Each is loaded into a comoving optical lattice. The lattices decelerate the momentum difference to $2n\hbar k$. Afterwards, when the paths cross, a Bragg diffraction acts as a beam splitter. Finally, the outputs are accelerated symmetrically to a splitting of $(2n + 4N)\hbar k$. To make the simultaneous accelerated lattices, one can, for example, superimpose two frequencies $\omega_1^{1,2}$ in one beam which are ramped as shown in Fig. 2(b). The difference frequencies in this example start at $(\omega_1^1 - \omega_2) = -(\omega_1^2 - \omega_2) = 8(2N + n)\omega_r$, and are ramped down to $8n\omega_r$. For Bragg diffraction, there is just one frequency in each beam, so that $\omega_1 = \omega_2$ in this specific reference frame. The figure also shows the laser intensity versus time (the intensities of

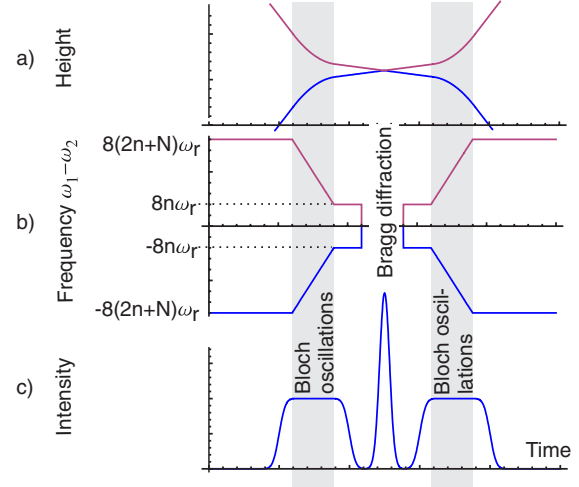


FIG. 2 (color online). Trajectories of the atom (a), laser frequencies (b), and laser intensities (c) during a BBB beam splitter.

the counterpropagating beams are proportional to each other) [24].

The realization of these ideas faces several challenges: For one, the simultaneous use of two optical lattices to accelerate populations coherently into different directions has never been demonstrated. Moreover, each BBB beam splitter uses four optical lattices and one Bragg diffraction, and a full interferometer consists of four beam splitters. Even if single accelerated lattices and Bragg diffractions have been shown to be coherent, the end-to-end coherence of a BBB beam splitter or a full interferometer may be very hard to realize. Moreover, interferometers with very high momentum transfer are prone to loss of interference contrast due to vibrational noise, even with state-of-the-art vibration isolation [11].

To avoid this loss of contrast, we use simultaneous conjugate interferometers (SCI) [12]. Two interferometers are run simultaneously, and their fringes are plotted against each other, forming an ellipse (Fig. 1). Common-mode phase fluctuations move the data around the ellipse, but do not affect the eccentricity, which is determined by the differential-mode phase. Ellipse-specific fitting [25] or Bayesian estimation [26] allows us to extract the differential phase independent of common-mode noise. Whereas the first and second beam splitter are common to our SCIs, the third and fourth are two superimposed BBB splitters, each addressing one interferometer according to the momentum of the atom (Fig. 1). Thus, the pair of SCIs even requires quadruple optical lattices, for a total of 24 optical lattices and 6 Bragg diffractions. Coherence of such an intricate atom-optics-system has rarely been demonstrated, if at all.

Our experiment uses a 1-m high atomic fountain of about 10^6 Cs atoms in the $F = 3$, $m_F = 0$ quantum state with a velocity distribution of 0.3 recoil velocities full width at half maximum (FWHM). It is based on a three-dimensional magneto-optical trap (MOT) with a moving

optical molasses launch and subsequent Raman sideband cooling in a comoving optical lattice [27].

Our laser system for driving Bloch oscillations and Bragg diffraction is based on a 6 W Ti:sapphire laser [12,28], stabilized with a red detuning of 16 GHz to the $F = 3 \rightarrow F' = 4$ transition in the cesium D2 manifold near 852 nm. An acousto-optical modulator AOM 1 (Fig. 3) is used for closed-loop amplitude control. To generate ω_1^{1-4} , AOM 2 is driven with up to 4 radio frequencies near 180 MHz (these frequencies are close enough so that the difference in deflection angle can be neglected). Phase shifts due to optical path length fluctuations are thus common to ω_1^{1-4} to a high degree. This is essential for the cancellation of vibrations between the conjugate interferometers. The beam at ω_2 is ramped using the double-passed AOM 4. Such ramping accounts for the free fall of the atoms, which changes the resonance condition in the laboratory frame at a rate of ~ 23 MHz/s. The two beams are brought to the experiment via two single-mode, polarization-maintaining fibers and collimated to an $1/e^2$ intensity radius of about 3 mm. The bottom beam has a maximum power of 1.15 W at the fiber output, the top beam a peak power of 1.6 W, or, respectively, 0.4 and 0.1 W per frequency in two and four-frequency operation. See Ref. [12] for more details.

An experimental sequence starts with launching the atoms to a 1-s vertical ballistic trajectory. The first 70 ms are used for preparing the atomic sample. After the experiment, the atoms are fluorescence detected as they pass a photomultiplier tube (PMT).

The Bragg pulses of our BBB beam splitters are Gaussian with a $1/\sqrt{e}$ half-width $\sigma \sim 20 \mu\text{s}$. Their intensity is adjusted for a 50% diffraction efficiency. The Bloch oscillation acceleration phase has a duration of 1–2 ms. The laser intensity is set sufficiently high for a Bloch oscillation efficiency of nearly 100% [14] and is adiabatically switched on and off with a rise time of several 100 μs . Figure 4 shows the PMT fluorescence signal of the population after one beam splitter versus time. Since the atoms reach the PMT at a time dependent on their velocity after the beam splitter, the x-axis gives the momentum transfer with a scaling of 0.7 ms/ $(\hbar k)$. The resolution of about $1\hbar k$ is determined by the spatial extent of

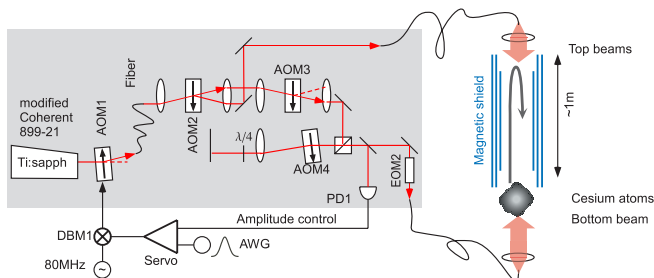


FIG. 3 (color online). Setup. Arbitrary waveform generator (AWG). $\lambda/4$: quarter-wave retardation plate. Double-balanced mixer (DBM).

the atomic sample, and the slots used for the detection beam and PMT. Figure 4 shows a momentum splitting of $88\hbar k$, of which $8\hbar k$ have been transferred by Bragg diffraction. The small peak in the middle is due to atoms which could not be diffracted.

A pair of interferometers is driven by combining BBB splitters in the way shown in Fig. 1. The population in the four outputs $a - d$ is detected by their fluorescence f_{a-d} . To take out fluctuations in the initial atom number, we define the normalized fluorescence $F_u = (f_a - f_b)/(f_a + f_b)$ of the upper interferometer and F_l in analogy for the lower interferometer. Figure 5 shows ellipses of the two interferometers, obtained by plotting their interference fringes F_u, F_l versus one another. Interferometers with momentum transfers between 12–24 $\hbar k$ are shown. The pulse separation time T (see Fig. 1) was between 2–10 ms, with little influence on contrast as expected for simultaneous interferometers [12]. We usually transferred (4–8) $\hbar k$ by Bragg diffraction; see Fig. 5. Even at the highest total splitting of 24 $\hbar k$, a contrast [29] of 15% is achieved, compared to 4% in the only previous instrument with such splitting (based on Bragg diffraction alone) [11]. This contrast is 30% of the theoretical value for Ramsey-Bordé interferometers [11,12].

The momentum splitting of 24 $\hbar k$ is currently limited by two technical issues. (i) The frequency ramps for driving Bloch oscillations were generated by a staircase approximation with at most 1024 steps. Large spans thus require a coarse step size, leading to loss of coherence. A better ramp generator will resolve this issue. (ii) Distortions of the wave fronts of the laser beam, caused by imperfect lenses, wave plates, and vacuum viewports, lead to loss of contrast as described in [12]. A mode-filtering cavity will alleviate this.

Outside of interferometers, Bloch oscillations have already been used to coherently transfer 8000 $\hbar k$ [15]. The BBB splitter thus opens up the door to substantial increases in atom-interferometer-sensitivity. One exciting application for such an ultrasensitive device is an atomic gravitational wave interferometric sensor (AGIS) [16]. Such a sensor could access the gravitational wave spectrum between 0.1–100 Hz, complementing the reach of optical interferometers such as LIGO and LISA. Sensing in this spectral region enables searches for white dwarf, black

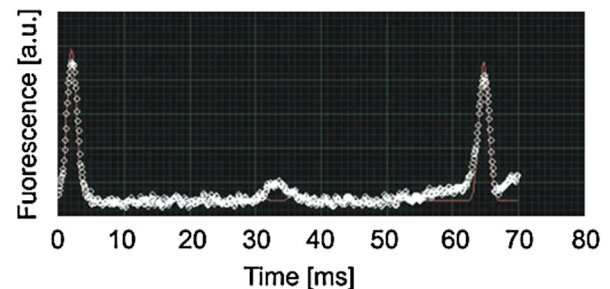


FIG. 4 (color online). Time-of-flight sheet of the output of an $88\hbar k$ beam splitter.

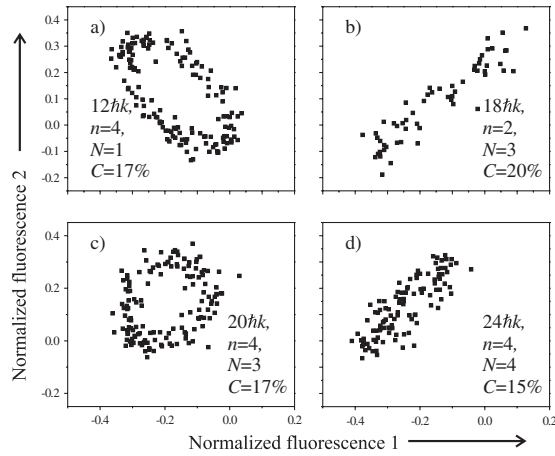


FIG. 5. Ellipses from simultaneous conjugate interferometers with BBB beam splitters. Total momentum transfer, Bragg diffraction order n , Bloch oscillation number N , and contrast C [29] are stated. All graphs are plotted using the same scale.

hole, and intermediate mass black hole binaries, or for the stochastic gravitational wave background from phase transitions in the early universe. A crucial ingredient of an AGIS is a momentum splitting of $100\hbar k$ or more; another is common-mode rejection of vibrations between simultaneous interferometers. Both common-mode rejection as well as large momentum transfer have already been demonstrated here. Other applications requiring extremely large enclosed areas include measuring the Lense-Thirring effect [17], or tests of the equivalence principle [18] and atom neutrality [19].

To summarize, we used Bloch oscillations and Bragg diffraction to demonstrate atom interferometers with a scalable momentum-space splitting Δp between the arms. Simultaneous Bloch oscillations and use of a single internal state [11] in both arms suppress systematic effects; simultaneous interferometers [12] suppress vibrational noise. Individual beam splitters reach $\Delta p = 88\hbar k$; interferometers with $\delta p = 24\hbar k$ reach 30% of their optimum contrast. This represents the highest momentum transfer realized to date in any light pulse atom interferometer [11], while substantially improving contrast. Most importantly, δp can be scaled up, as it is no longer limited by the available laser power. This will be instrumental in realizing several proposed landmark experiments [16–20]. For example, ours is the first experimental demonstration of atom interferometers that can be scaled up for gravitational wave detection.

We are indebted to Jason Hogan, Mark Kasevich, Tim Kovachy, and Shau-yu Lan for discussions. This material is based upon work supported by the National Science

Foundation under Grant No. 0400866. S.H. and H.M. thank the Alexander von Humboldt Foundation.

*Also at Physics Department, Stanford University, 382 Via Pueblo Mall, Stanford, CA 94305, USA.
hm@berkeley.edu

- [1] A.D. Cronin, J. Schmiedmayer, and D.E. Pritchard, arXiv:0712.3703v1 [Rev. Mod. Phys. (to be published)].
- [2] A. Peters, K. Y. Chung, and S. Chu, *Nature (London)* **400**, 849 (1999).
- [3] D. S. Weiss, B. C. Young, and S. Chu, *Phys. Rev. Lett.* **70**, 2706 (1993); M. Weitz, B. C. Young, and S. Chu, *ibid.* **73**, 2563 (1994).
- [4] A. Wicht *et al.*, *Phys. Scr.* **T102**, 82 (2002).
- [5] P. Cladé *et al.*, *Phys. Rev. Lett.* **96**, 033001 (2006); *Phys. Rev. A* **74**, 052109 (2006); M. Cadoret *et al.* arXiv:0809.3177.
- [6] M. J. Snadden *et al.*, *Phys. Rev. Lett.* **81**, 971 (1998).
- [7] J. B. Fixler *et al.*, *Science* **315**, 74 (2007).
- [8] G. Lamporesi *et al.*, *Phys. Rev. Lett.* **100**, 050801 (2008).
- [9] H. Müller *et al.*, *Phys. Rev. Lett.* **100**, 031101 (2008).
- [10] D. M. Giltner, R. W. McGowan, and S. A. Lee, *Phys. Rev. Lett.* **75**, 2638 (1995); A. Miffre *et al.*, *Eur. Phys. J. D* **33**, 99 (2005).
- [11] H. Müller *et al.*, *Phys. Rev. Lett.* **100**, 180405 (2008).
- [12] S.-w. Chiow, S. Herrmann, S. Chu, and H. Müller, arXiv:0901.1819.
- [13] H. Müller, S.-w. Chiow, and S. Chu, *Phys. Rev. A* **77**, 023609 (2008).
- [14] E. Peik *et al.*, *Phys. Rev. A* **55**, 2989 (1997).
- [15] G. Ferrari *et al.*, *Phys. Rev. Lett.* **97**, 060402 (2006).
- [16] S. Dimopoulos *et al.*, *Phys. Rev. D* **78**, 122002 (2008).
- [17] A. Landragin *et al.*, in *Optics in Astrophysics*, edited by R. Foy and F.C. Foy, NATO Science Series II Vol. 198 (Springer, Berlin, Germany, 2005), p. 359.
- [18] S. Dimopoulos *et al.*, *Phys. Rev. Lett.* **98**, 111102 (2007); *Phys. Rev. D* **78**, 042003 (2008).
- [19] C. Lämmerzahl, A. Macias, and H. Müller, *Phys. Rev. A* **75**, 052104 (2007); A. Arvanitaki *et al.*, *Phys. Rev. Lett.* **100**, 120407 (2008).
- [20] H. Müller *et al.*, *Appl. Phys. B* **84**, 633 (2006).
- [21] J. Hecker-Denschlag *et al.*, *J. Phys. B* **35**, 3095 (2002).
- [22] P. Cladé *et al.*, *Phys. Rev. Lett.* **102**, 240402 (2009).
- [23] J. Hogan and T. Kovachy (private communications).
- [24] For simplicity, the intensity as averaged over a period of the beat note between the two frequencies is shown.
- [25] G. T. Foster, J. B. Fixler, J. M. McGuirk, and M. A. Kasevich, *Opt. Lett.* **27**, 951 (2002).
- [26] J. K. Stockton, X. Wu, and M. A. Kasevich, *Phys. Rev. A* **76**, 033613 (2007).
- [27] P. Treutlein, K. Y. Chung, and S. Chu, *Phys. Rev. A* **63**, 051401(R) (2001).
- [28] S.-w. Chiow *et al.*, *Opt. Express* **17**, 5246 (2009).
- [29] Determined as the average of the radii in the x and y direction of the fitted [25] ellipse.